J IRAN CHEM SOC
DOI 10.1007/s13738-013-0400-8

ORIGINAL PAPER

Magnetic nanoparticles-supported tungstosilicic acid: as an efficient magnetically separable solid acid for the synthesis of benzoazoles in water

Ali Khalafi-Nezhad · Farhad Panahi · Reza Yousefi · Sina Sarrafi · Yasaman Gholamalipour

Received: 24 September 2013 / Accepted: 22 December 2013

Abstract The magnetic nanoparticles-supported tungstosilicic acid (TSAMNP) was found to be a highly efficient solid acid for the synthesis of benzoazoles in water. TSAMNP catalyst was achieved by the immobilization of tungstosilicic acid [$H_4(W_{12}SiO_{40})$] species on the silica core–shell magnetic nanoparticles (Fe_3O_4@SiO_2). A variety of aldehydes were successfully condensed with 1,2-diaminobenzene, 2-aminophenol and 2-aminothiophenol in water as a green solvent to synthesize benzoazoles in good-to-excellent yields. TSAMNP catalyst was easily separated from the reaction mixture and reused several times without any loss of efficiency.

Keywords Magnetic nanoparticles · Heteropoly acids · Tungstosilicic acid · Benzoazoles · Water

Introduction

In both academic researches and industries, heteropoly acids (HPAs) have been widely used as catalyst in a large number of organic reactions for fine chemical synthesis of many materials [1–5]. The advantages of these catalysts in organic transformations are mentioned as follows: high catalytic performance, strong acidity, selectivity to a particular reaction product by selective stabilization of the reaction intermediate, corrosiveness, safety, and lower waste [6]. One of the most important approaches to improve their applicability in organic reactions is their immobilization on a recyclable support. As a result, supported heteropoly acids (SHPAs) have been introduced as economically and environmentally benign catalysts in the recent years [7]. The immobilization of HPAs on different type of supports has been employed [8–10]. However, the activity and selectivity of supported catalysts are decreased frequently, due to a significant reduction in reactant diffusion rate to the surface of catalyst [11]. The aforementioned problem can be resolved to some extent by selecting the very small size ranges of the support. Because of nanometer size-range of nanoparticles which allow their surface areas to increase dramatically, these materials are reasonable potential candidate supports [12]. Moreover, nanoparticles are dispersible in solution, forming emulsion which further increases the diffusion rate [13]. In addition, reactants in solution have easy access to the active sites on the surface of nanomaterial. However, when the size of support is decreased to nanometer scale, a simple filtration method cannot overcome the big obstacle of catalyst separation from the reaction media. As a solution, the efforts have been focused on magnetic recyclable supports such as magnetic nanoparticles (MNPs) [14]. When MNPs are used as support, both reactivity and reusability (catalyst can be separated from reaction condition using an external magnetic field) could be improved. Thus, by immobilization of HPAs on MNPs it is possible to prepare a highly efficient solid acid based on HPAs for application in organic reactions [15].

In this study, we applied a MNPs-supported tungstosilicic acid catalyst as a highly efficient and easy separable solid acid for the synthesis of benzoazoles in water as a green solvent. It is noteworthy that, the benzoazole ring systems are important pharmacophores in medicinal

A. Khalafi-Nezhad (✉) · F. Panahi · S. Sarrafi · Y. Gholamalipour
Department of Chemistry, College of Sciences, Shiraz University, 71454 Shiraz, Iran
e-mail: khalafi@chem.susc.ac.ir

R. Yousefi
Protein Chemistry Laboratory (PCL), Department of Biology, College of Sciences, Shiraz University, Shiraz, Iran

Published online: 18 January 2014

chemistry and modern drug discovery [16–18]. A large number of their derivatives have been found to exhibit various biological activities such as anti inflammatory, antifungal, antibacterial, anthelminthic, analgesic, antiviral, anti trypanosomatid, anticonvulsant, cytotoxic, antidiabetics and antiulcer activities [19–23]. Some of the benzoazole-based compounds have interesting photophysical properties, and they are widely used in organic electronic devices [24–28]. However, some of the reported methods for the synthesis of this class of compounds suffer from disadvantage of use of toxic and unrecyclable catalysts and solvents, prolonged reaction times, harsh reaction conditions and difficult work-up procedures [29–43].

Results and discussion

In the current study, TSAMNP catalyst was prepared using immobilization of tunstosilicic acid (as a stable and reactive Keggin type HPA) [44] on the Fe_3O_4-modified silica nanoparticles (Fe_3O_4@SiO_2) as shown in Scheme 1. Fe_3O_4 nanoparticles were synthesized by a reported thermal decomposition method [45]. The synthesized Fe_3O_4 nanoparticles were coated by silica via a sol–gel process to obtain Fe_3O_4@SiO_2 [46]. The silica shell not only prevents the aggregation of MNPs during the catalyst preparation process, it also provides an easy access to the connection of $H_4(W_{12}SiO_{40})$ species to the surface of MNPs. The TSAMNP catalyst was obtained from the reaction of $H_4(W_{12}SiO_{40})$ and the Fe_3O_4@SiO_2 according to the procedure in the literature [47].

To confirm the synthesis of TSAMNP catalyst its structure was characterized using both microscopic analysis and spectroscopic techniques. The analytical percentage of elements for TSAMNP using energy dispersive X-ray (EDS) was obtained as Fe (42.36), W (17.44), Si (18.31) and O (21.89). Using the EDS analysis, the amount of protons in TSAMNP was obtained about 0.225 mmol g^{-1}. The comparison between FT-IR spectra of $H_4(W_{12}SiO_{40})$, Fe_3O_4@-SiO_2 nanoparticles, and TSAMNP shows that TSAMNP catalyst was generated according to our procedure (Fig. 1). The broad band around 1,200–1,050 cm^{-1}, corresponding to asymmetric stretching of Si–O–Si bond was seen in both Fe_3O_4@SiO_2 nanoparticles and TSAMNP catalyst [48]. Also peaks at around 500 cm^{-1} can be attributed to the bending vibration of the Si–O–Si bonds [8]. The broad absorption band around 3500 cm^{-1} is the absorption of -OH bond on the surface of all materials. The peaks around 1,700–1,800 cm^{-1} which are existed in the structure of $H_4(W_{12}SiO_{40})$ can be seen in the FT-IR of TSAMNP. Importantly, the characteristic bands at 1025, 995, 915, 880, and 769 cm^{-1} correspond to W=O symmetrical and asymmetrical, Si–O asymmetrical, W–Ob–W asymmetrical, and W–Oc–W asymmetrical, respectively [49]. The presence of these bands strongly reveals that the primary structure of $H_4(W_{12}SiO_{40})$ species is preserved even after anchoring to MNP support.

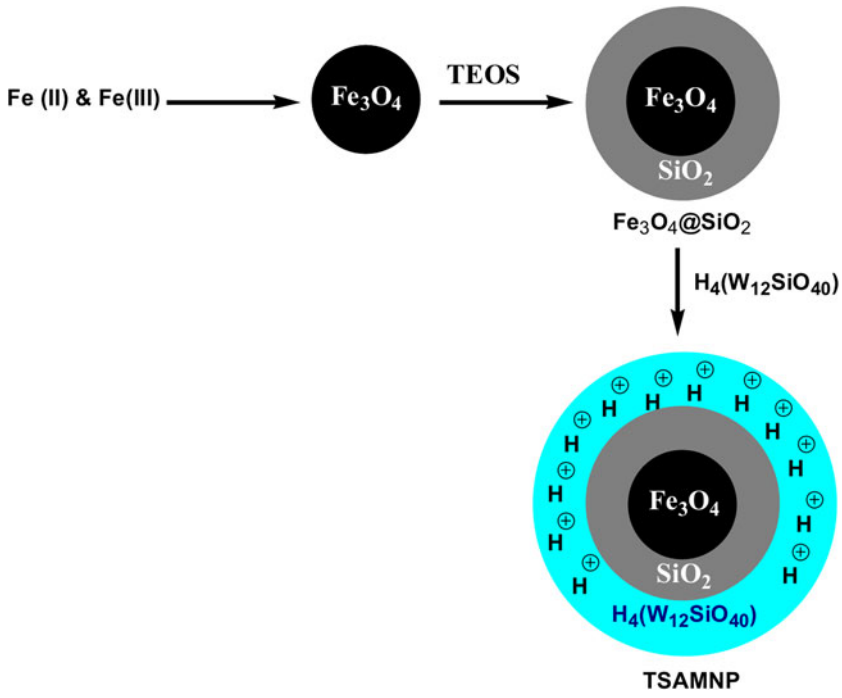

Scheme 1 The synthetic route for the preparation of TSAMNP catalyst

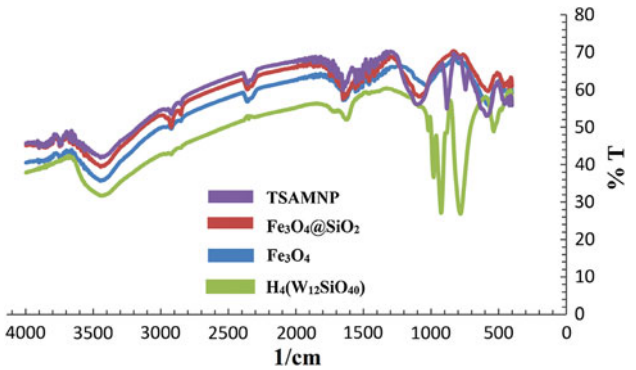

Fig. 1 The FT-IR spectra of TSAMNP, Fe_3O_4@SiO_2, Fe_3O_4, and $H_4(W_{12}SiO_{40})$

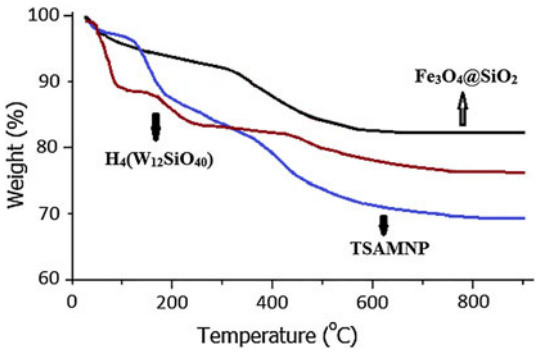

Fig. 2 The TGA of pure $H_4(W_{12}SiO_{40})$, Fe_3O_4@SiO_2 nanoparticles, and TSAMNP

A comparison between the thermal gravimetric analysis (TGA) curves of pure $H_4(W_{12}SiO_{40})$, Fe_3O_4@SiO_2 nanoparticles, and TSAMNP catalyst is depicted in Fig. 2.

As shown in Fig. 1, the TGA of TSAMNP shows 2.7 % weight loss within a temperature range of 150–170 °C which is due to the loss of adsorbed water molecules. Furthermore, it shows 6.7 % weight loss at 180–210 °C due to the loss of water of crystallization and 13.1 % weight loss at 300–450 °C, which is due to the decomposition of anchored heteropoly acid.

To further study the immobilization of the $H_4(W_{12}SiO_{40})$ species into MNPs, TSAMNP catalysts were characterized using transmission electron microscopy (TEM) and x-ray diffraction pattern (XRD). The TEM image of TSAMNP catalyst is depicted in Fig. 3. According to both TEM image (Fig. 3) and histogram, the average diameter of TSAMNP particles is estimated to be 45 nm. TEM images of TSAMNP catalyst show the near spherical TSAMNP particles which are produced during preparation process. To further explore the chemically modification of the MNPs with TSA, the morphology of the catalyst was studied using XRD. The XRD pattern of TSAMNP catalyst (Fig. 4) shows that the catalyst was synthesized successfully using our methodologies. The peaks are indexed as the (220),

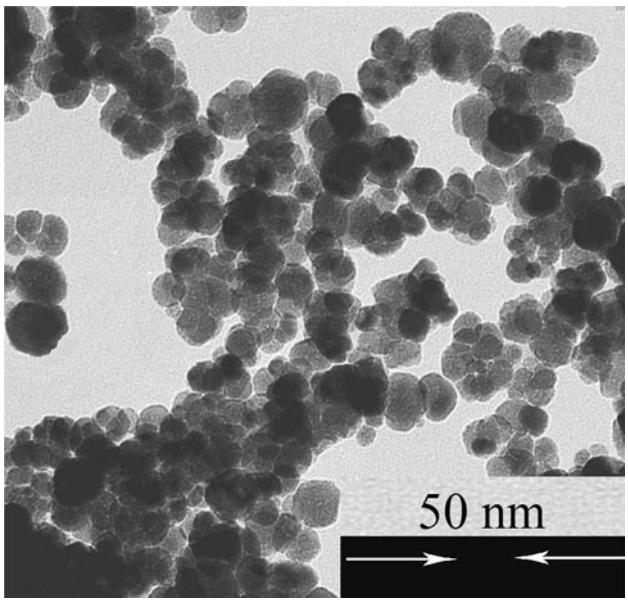

Fig. 3 The TEM image of TSAMNP

(311), (400), (422), (511) and (440) planes of the Fe_3O_4 nanoparticles [50].

To evaluate the catalytic performance of TSAMNP, we checked the synthesis of benzoazoles (benzoxazoles, benzoimidazoles and benzothiazoles) via the condensation of aldehydes with benzene1,2-diamine, 2-aminophenol or 2-aminothiophenol as an acid catalyzed process. To optimize the conditions for maximum yields of desired products, the effect of different reaction parameters such as catalyst loading, temperature, solvent and reaction time were investigated. So, the reaction between 2-aminophenol (**1**) and benzaldehyde (**2**) as a model was tested under different conditions, and the results are depicted in Table 1.

The results indicated that TSAMNP catalyst can be applied as a powerful, green and magnetically separable catalyst for the synthesis of benzoazoles under green conditions. As it is shown in Table 1 by varying the type of solvent the yield of the desired product did not change significantly in comparison with water (Table 1, entries 9–12). Also with increasing the amount of catalyst the yield of product remained unchanged (Table 1, entry 13). Furthermore, as a result of reducing the amount of catalyst a reduction was observed in the yield of product (Table 1, entry 14). These results show that the catalytic amount of TSAMNP is applicable for this reaction. Thus, the simple system, TSAMNP (0.05 g), H_2O as solvent, and reflux temperature of water, was chosen as the optimized reaction conditions (Table 1, entry 6). To determine the scope of this protocol, various benzoazoles were synthesized under the optimized conditions, and the results are summarized in Table 2.

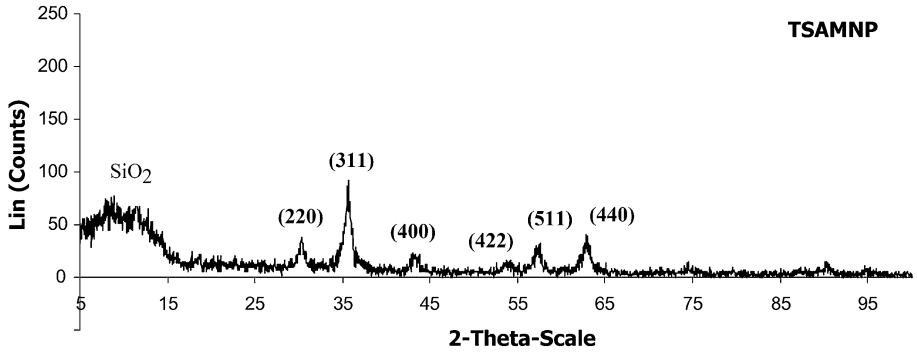

Fig. 4 The XRD spectra of TSAMNP

Table 1 The study of different conditions for the synthesis of 2-phenylbenzo[*d*]oxazole (**3a**) using TSAMNP as catalyst

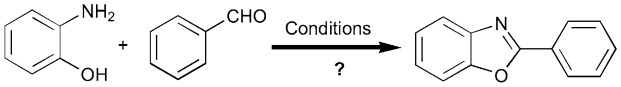

(1a) (2a) (3a)

Entry	Catalyst	Solvent	Temp./ °C	Time (h)	Yield (%)[a]
1	–	–	r.t.	24	0
2	–	–	100	12	15
3	–	H_2O	Reflux	12	21
4	Fe_3O_4@SiO_2	H_2O	Reflux	12	32[b]
5	$H_4(W_{12}SiO_{40})$	H_2O	Reflux	12	81[c]
6	TSAMNP	H_2O	Reflux	5	95
7	TSAMNP	–	r.t.	24	19
8	TSAMNP	–	100	12	61
9	TSAMNP	EtOH	Reflux	12	65
10	TSAMNP	$CHCl_3$	Reflux	12	76
11	TSAMNP	Toluene	100	12	68
12	TSAMNP	DMSO	100	12	84
13	TSAMNP	H_2O	Reflux	12	96[d]
14	TSAMNP	H_2O	Reflux	5	84[e]

Reaction conditions: 2-aminophenole (1.1 mmol), benzaldehyde (1 mmol), catalyst (0.05 g), and solvent (5 mL)

[a] Isolated yield

[b] 0.1 g of Fe_3O_4@SiO_2 was used

[c] 0.05 g of $H_4(W_{12}SiO_{40})$ was used

[d] 0.06 g of catalyst was used

[e] 0.04 g of catalyst was used

The results in Table 2 revealed that, TSAMNP is an active and efficient catalyst for the synthesis of benzoazoles in water. The reaction condition is quite broad with respect to the substrates examined, providing the desired benzoazoles with good-to-excellent yields. As clearly shown in Table 2, TSAMNP catalyst can be used for aromatic aldehydes with electron-withdrawing and electron-

Table 2 The synthesis of benzoazoles in the presence of TSAMNP as a magnetically separable solid acid catalyst in water

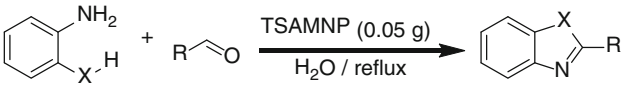

X = O, S, NH 3a-z

Entry	X	R	Time (h)	Yield (%)[a]
3a	O	Ph	5	95
3b	S	Ph	3	97
3c	NH	Ph	6	94
3d	O	3-OH-Ph	5	93
3e	NH	4-CN-Ph	3	97
3f	NH	3-NO_2-Ph	4	95
3g	O	4-OH-Ph	6	91
3h	S	4-OH-Ph	6	93
3i	NH	4-OMe-Ph	6	91
3j	S	2-Me-Ph	8	90
3k	S	4-OMe-Ph	6	92
3l	O	2-Me-Ph	8	89
3m	O	Ph-CH_2-	8	86
3n	O	Et	10	84
3o	S	Et	10	85
3p	S	2-Cl-Ph	8	91
3q	O	2-Cl-Ph	8	90
3r	NH	2-Cl-Ph	8	92
3s	S	2,6-F-Ph	8	88
3t	NH	2-pyridinyl	8	87
3u	NH	2,6-Cl-Ph	8	88
3v	O	4-Br-Ph	5	91
3w	S	4-Br-Ph	5	93
3x	NH	4-Cl-Ph	5	93
3y	S	Ph-CH_2-	6	88
3z	NH	4-Me-Ph	6	90

Reaction conditions: 2-aminophenol/-thiphenol/benzene-1,2-diamine (1.1 mmol), aldehyde (1.0 mmol), TSAMNP (0.05 g), H_2O (5 mL) under reflux conditions

[a] Isolated yield

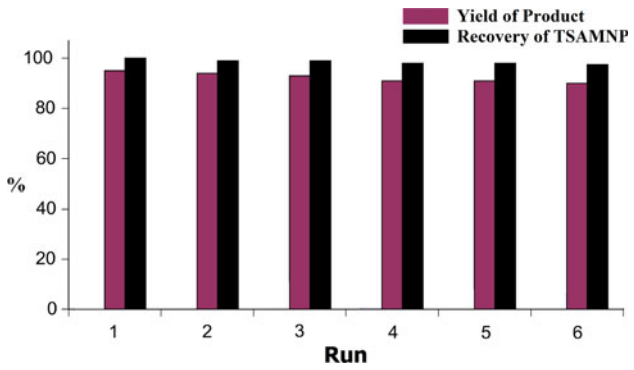

Fig. 5 The reusability of the TSAMNP catalyst in synthesis of benzoazoles in water

donating groups. Moreover, aliphatic aldehydes can be used under the same reaction conditions.

For practical applications of a heterogeneous catalyst, the level of reusability is a very important parameter. Thus, the possibility of recycling the catalyst was tested using the model reaction under optimized conditions. The recycled catalyst could be reused at least for five times without any treatment in its catalytic activity (Fig. 5).

Since leaching of the active species from the support makes the catalyst unattractive, the stability study of a heterogeneous catalyst is necessary. Thus, the leaching of TSA species from the magnetic support was checked. After six times of reusability we checked the W content of TSAMNP catalyst using EDX analysis, and the results were shown that <0.1 % of W was lost. This result was also confirmed by ICP using hot filtration test. In an experiment, when the reaction between benzaldehyde with 2-aminophenol was completed, the hot filtration had been accomplished and the ICP analysis of the aqueous solution showed <1 ppm of W. Considering these results, it can be concluded that there is a small amount of TSA species leaching from the magnetic support and the present catalyst is truly heterogeneous in nature. These results are in good agreements with the catalytic activity of the TSAMNP after each recovery.

Experimental

General

Chemicals were purchased from Fluka and Aldrich chemical companies and used as received. FT-IR spectroscopy (Shimadzu FT-IR 8300 spectrophotometer), was employed for characterization of the catalyst and synthesized compounds. The transmission electron microscopy (TEM) was obtained using TEM apparatus (CM-10-philips, 100 kV). The thermogravimetry analysis (TGA) of the samples was analyzed using a labmade TGA instrument. For recorded ^{1}H NMR spectra, we used a Brucker (250MHZ) Avance DRX in pure deuterated DMSO-d_6 and $CDCl_3$ solvents with tetramethylsilane (TMS) as the internal standard. Mass spectra were recorded on a FINNIGAN-MAT 8430 mass spectrometer operating at 70 eV. Melting points were determined in open capillary tubes in a Barnstead Electrothermal 9100 BZ circulating oil melting point apparatus. The reaction monitoring was accomplished by TLC on silica gel PolyGram SILG/UV254 plates. Column chromatography was carried out on columns of silica gel 60 (70–230 mesh).

Preparation of Fe_3O_4 nanoparticles

Magnetic nanoparticles were prepared via the co-precipitation of Fe(III) and Fe(II) ions in the presence of sodium hydroxide. For this purpose, in a canonical flask, a mixture of $FeCl_2.2H_2O$ (16 mmol, 2.6 g) and $FeCl_3{\cdot}6H_2O$ (30 mmol, 8.1 g) was dissolved in 100 mL of deionized water. Then, the 3 M aqueous solution of NaOH was added drop-wise (in a period of 5 min) at 40 °C until the pH of the resulting mixture increased to 11. Subsequently, the temperature of mixture was increased to 80 °C and the solution was stirred for 20 min. The magnetic nanoparticles as a dark solid were isolated from the solution by magnetic separation and washed with deionized water until pH 7 reached. Obtained material was dried under reduced pressure for 12 h, and Fe_3O_4 nanoparticles were obtained as a brown powder.

Preparation of $Fe_3O_4@SiO_2$ nanoparticles

$Fe_3O_4@SiO_2$ nanoparticles were prepared based on the literature with some modifications. To a mixture of cyclohexane (250 mL), 1-hexanol (50 mL), triton X-100 (80 mL) and water (25 mL), Fe_3O_4 nanoparticles (2 g) was added and the mixture stirred by a mechanical stirrer under N_2 atmosphere for 30 min. Tetraethyl orthosilicate (TEOS) (20 mL) was added to the mixture and the solution stirred for additional 12 h at 30 °C. After the specified time, ammonia (saturated solution in water) (18 mL) was added and the solution stirred continuously for another 12 h. The precipitate was washed with ethanol (10 mL, 3 times) and collected using an external magnetic field. The obtained gray product was dried under reduced pressure overnight and $Fe_3O_4@SiO_2$ obtained as a gray solid.

Preparation of magnetic nanoparticles-supported tungstosilicic acid (TSAMNPs)

The TSAMNP was prepared using an impregnation method. For this, $Fe_3O_4@SiO_2$ nanoparticles (2.0 g) were mixed with a solution of tungstosilicic acid (0.57 g, 0.2 mmol) in deionized water (25 mL). The obtained

mixture was stirred at 60 °C for 1 h using a mechanical stirrer. Then the mixture was filtered and washed by distilled water (20 mL, 2 times). The filtrate was dried at 80 °C for 2 h, then calcined at 150 °C for 5 h and TSAMNP was obtained as a dark solid powder.

General producer for the synthesis of benzoxazoles in the presence of TSAMNP as a solid acid catalyst

To the suspension of aldehyde (1 mmol) and 2-aminophenol/-thiphenol/benzene-1,2-diamine (1 mmol) in water (5 mL), TSAMNP (0.05 g, 12 mol % based on H^+ content) was added and the resulting mixture heated to 70 °C for 5 h. Then the reaction was followed by TLC. After completion of the reaction, the mixture was cooled down to room temperature and the catalyst magnetically separated from the reaction mixture and washed with diethyl ether (10 mL, 2 times) followed by deionized and oxygen-free water (10 mL, 2 times), dried under reduced pressure and reused for the next run. The aqueous phase was extracted with diethyl ether (10 mL, 2 times) and the combined organic phases dried over Na_2SO_4. The benzoazole product was purified by column chromatography (hexane/ethyl acetate) to obtain the desired purity.

Spectral data of synthesized compounds

2-phenyl-1,3-benzoxazole (3a): Yield 95 %, white crystals, mp: 103–104 °C (Lit. [48] mp 103 °C). IR (KBr): $\overline{V}$ = 3,049, 1,608, 1,547, 1,483, 1,445, 1,238, 1,047, 1,013, 920, 744, 692 cm^{-1}. ^{1}H-NMR (250 MHz, $CDCl_3$/TMS) δ (ppm): 7.19–7.22 (m, 2H), 7.36–7.41 (m, 4H), 7.61–7.65 (m, 1H), 8.11–8.15 (m, 2H). ^{13}C-NMR (62.9 MHz, $CDCl_3$/TMS) δ (ppm): 110.6, 120.0, 124.6, 125.1, 127.1, 127.6, 128.9, 131.5, 142.1, 150.7, 163.0.

2-phenyl-1,3-benzothiazole (3b): Yield 97 %, white crystals, mp: 113–114 °C (Lit. [49] mp 112–114 °C). IR (KBr): $\overline{V}$ = 3,060, 1,472, 1,431, 960, 762, 687 cm^{-1}. ^{1}H-NMR (250 MHz, $CDCl_3$/TMS) δ (ppm): 7.35–7.38 (m, 1H) 7.47–7.51 (m, 4H), 7.88–7.91 (m, 1H) 8.1–8.13 (m, 3H). ^{13}C-NMR (62.9 MHz, $CDCl_3$/TMS) δ (ppm): 121.6, 123.2, 125.2, 126.3, 127.6, 129.0, 131.0, 133.6, 135.1, 154.1, 168.1.

2-phenylbenzimidazole (3c): Yield 94 %, white crystals; mp 295–296 °C (Lit. [51] mp 295 °C). IR (KBr): $\overline{V}$ = 3,440, 1,620, 1,591, 1,450, 1,412, 1,315, 1,277, 1,113, 742, 694 cm^{-1}. ^{1}H-NMR (250 MHz, DMSO-d_6/TMS) δ (ppm): 7.14–7.25 (m, 2H), 7.44–7.61 (m, 5H), 8.20 (d, J = 7.2 Hz, 2H), 12.94 (s, 1H). ^{13}C-NMR (62.9 MHz, DMSO-d_6/TMS) δ (ppm): 122.1, 126.4, 128.4, 128.9, 129.2, 129.8, 130.1, 151.2.

3-(1,3-Benzoxazol-2-yl)phenol (3d): Yield 93 %, white solid; mp: 237–238 °C. IR (KBr): $\overline{V}$ = 3,125, 3,092, 1,603, 1,555, 1,454, 1,301, 750 cm^{-1}. ^{1}H-NMR (250 MHz, DMSO-d_6/TMS) δ (ppm): 7.01 (dd, J = 7.3, 1.2 Hz, 1H), 7.30–7.40 (m, 3H), 7.60 (d, J = 5.8 Hz, 2H), 7.67–7.76 (m, 2H). ^{13}C-NMR (62.9 MHz, DMSO-d_6/TMS) δ (ppm): 110.7, 113.6, 118.0, 119.0, 119.6, 124.7, 125.3, 127.4, 130.3, 141.4, 150.1, 157.8, 162.3.

4-(1H-1,3-benzimidazol-2-yl)benzonitrile (3e): Yield 97 %, white solid, mp: 262–263 °C. IR (KBr): $\overline{V}$ = 3,420, 3,050, 2,915, 2,220, 1,600, 1,450, 1,410, 840, 750 cm^{-1}. ^{1}H-NMR (250 MHz, DMSO-d_6/TMS) δ (ppm): 7.23–768 (m, 4H), 8.00 (d, J = 8.1 Hz, 2H), 8.32 (d, J = 8.1 Hz, 2H). ^{13}C-NMR (62.9 MHz, DMSO-d_6/TMS) δ (ppm): 111.7, 111.8, 118.6, 119.3, 122.2, 123.3, 127.0, 132.9, 134.2, 149.3.

2-(3-nitrophenyl)-1H-1,3-benzimidazole (3f): Yield 95 %, pale yellow solid; mp: 202.5 °C (Lit. [52] mp 200–202 °C). IR (KBr): $\overline{V}$ = 3,440, 3,080, 1,530, 1,350, 730 cm^{-1}. ^{1}H-NMR (250 MHz, $CDCl_3$) δ (ppm): 7.24–7.31 (m, 2H), 7.61–7.67 (m, 3H), 8.25 (d, J = 8.4 Hz, 1H), 8.42 (d, J = 7.8 Hz, 1H), 8.77 (t, J = 1.8 Hz, 1H). ^{13}C-NMR (62.9 MHz, DMSO-d_6/TMS) δ (ppm): 116.0, 120.8, 122.7, 124.2, 130.6, 131.6, 132.4, 136.9, 148.3, 149.0.

2-(3-nitrophenyl)-1H-1,3-benzimidazole (3g): Yield 91 %, white solid; mp: 259–260 °C. IR (KBr): $\overline{V}$ = 3,060, 3,000, 1,600, 1,480, 1,430, 1,280, 1,250, 1,220, 1,170, 830, 760 cm^{-1}. ^{1}H-NMR (250 MHz, DMSO-d_6/TMS) δ (ppm): 6.97 (d, J = 8.7 Hz, 2H), 7.27–7.33 (m, 2H), 7.61–7.72 (m, 2H), 8.01 (d, J = 8.7 Hz, 2H), 10.35 (s, 1H). ^{13}C-NMR (62.9 MHz, DMSO-d_6/TMS) δ (ppm): 115.3, 121.3, 122.4, 124.5, 129.8, 34.0, 134.5, 147.0, 155.2, 166.1, 168.0.

4-(1,3-benzothiazol-2-yl)phenol (3h): Yield 93 %, white solid, mp: 226–228 °C (Lit. [53] mp 227 °C). IR (KBr): $\overline{V}$ = 3,090, 1,600, 1,460, 1,440, 1,290, 1,230, 1,170, 970, 830, 746 cm^{-1}. ^{1}H-NMR (250 MHz, DMSO-d_6/TMS) δ (ppm): 6.97 (d, J = 8.5 Hz, 2H), 7.31 (t, J = 7.4 Hz, 1H), 7.42–7.45 (m, 1H), 7.92–7.99 (m, 4H), 10.31 (s, 1H). ^{13}C-NMR (62.9 MHz, DMSO-d_6/TMS) δ (ppm): 116.1, 121.9, 122.2, 123.5, 124.1, 126.2, 128.6, 134.2, 153.7, 160.5, 167.5.

2-(4-methoxyphenyl)benzimidazole (3i): Yield 91 %, white solid, mp: 226–228 °C (Lit. [54] mp 226–227 °C). IR (KBr): $\overline{V}$ = 3,440, 3,060, 2,950, 1,610, 1,500, 1,480, 1,450, 1,435, 1,400, 1,255, 1,180, 740 cm^{-1}. ^{1}H-NMR (250 MHz, DMSO-d_6/TMS) δ (ppm): 3.78 (s, 3H), 7.10 (d, J = 8.8 Hz, 2H), 7.16 (q, J = 3.0 Hz, 2H), 7.50 (m, 2H), 8.12 (d, J = 8.8 Hz, 2H), 12.76 (s, 1H). ^{13}C-NMR (62.9 MHz, DMSO-d_6/TMS) δ (ppm): 55.2, 111.0, 114.3, 118.4, 121.5, 122.0, 122.6, 128.0, 151.3, 160.5.

2-(2-methylphenyl)-1,3-benzothiazole (3j): Yield 90 %, white solid, mp: 54–55 °C (Lit. [53] mp 53–54 °C). IR (KBr): $\overline{V}$ = 3,060, 2,930, 1,475, 1,430, 950, 760, 720 cm^{-1}. ^{1}H-NMR (250 MHz, $CDCl_3$/TMS) δ (ppm): 2.8 (s, 3H), 8.26 (d, J = 8.1 Hz, 1H), 7.97 (d, J = 7.9 Hz, 1H), 7.90 (d, J = 7.2 Hz, 1H), 7.63–7.56 (m, 1H), 7.36–7.50 (m, 4H). ^{13}C-NMR (62.9 MHz, $CDCl_3$/TMS) δ (ppm): 21.3, 121.4, 123.5, 124.7, 126.2, 129.7, 130.4, 131.7, 133.1, 135.6, 137.3, 153.9, 168.0.

2-(4-methoxyphenyl)-1,3-benzothiazole (3k): Yield 92 %, white crystals, mp: 122–123 °C (Lit. [49] mp 1,120–121 °C).IR (KBr): $\overline{V}$ = 3,060, 2,990, 1,600, 1,480, 1,433, 1,260, 1,220, 1,170, 1,020, 960, 830, 760 cm^{-1}. ^{1}H-NMR (250 MHz, $CDCl_3$/TMS) δ (ppm): 3.71 (s, 3H), 6.84 (d, J = 8.85 Hz, 2H), 7.16–7.36 (m, 2H), 7.71 (d, J = 7.9 Hz, 1H), 7.86–7.9 (m, 3H). ^{13}C-NMR (62.9 MHz, $CDCl_3$/TMS) δ (ppm): 55.4, 114.4, 121.5, 122.8, 124.8, 126.2, 129.1, 134.8, 154.2, 161.9, 167.9.

2-(2-methylphenyl)-1,3-benzoxazole (3l): Yield 89 %, white solid, mp: 80–82 °C (Lit. [55] mp 81–82 °C). IR (KBr): $\overline{V}$ = 3,050, 2,960, 1,610, 1,540, 1,445, 1,240, 1,030, 750 cm^{-1}. ^{1}H-NMR (250 MHz, $CDCl_3$/TMS) δ (ppm): 2.65 (s, 3H), 7.12–7.18 (m, 5H), 7.37–7.42 (m, 1H), 7.61–7.67 (m, 1H), 7.99–8.03 (m, 1H). ^{13}C-NMR (62.9 MHz, $CDCl_3$/TMS) δ (ppm): 22.3, 110.5, 120.2, 124.4, 125.0, 126.2, 129.9, 130.9, 131.8, 138.9, 142.2, 150.3, 163.4.

2-benzyl-1,3-benzoxazole (3m): Yield 86 %, colorless liquid, IR (neat): $\overline{V}$ = 3,060, 3,030, 2,925, 1,610, 1,570, 1,490, 1,455, 1,430, 1,240, 1,145, 855, 920, 845, 750, 720 cm^{-1}. ^{1}H-NMR (250 MHz, $CDCl_3$/TMS) δ (ppm): 4.28 (s, 2H) 7.27–7.45 (m, 8H), 7.72–7.76 (m, 1H). ^{13}C NMR (62.9 MHz, $CDCl_3$/TMS) δ (ppm): 35.27, 110.5, 119.8, 124.2, 124.7, 127.6, 128.9, 129.0, 134.8, 141.4, 151.1, 165.2

2-ethyl-1,3-benzoxazole (3n): Yield 84 %, colorless liquid. IR (neat): $\overline{V}$ = 3,660, 2,930, 2,930, 1,610, 1,570, 1,460, 1,240, 1,160, 750 cm^{-1}. ^{1}H-NMR (250 MHz, $CDCl_3$/TMS) δ (ppm): 1.38 (t, J = 7.6 Hz, 3H), 2.89 (q, J = 7.6 Hz, 2H), 7.17–7.29 (m, 2H), 7.36–7.43 (m, 1H), 7.57–7.63 (m, 1H). ^{13}C-NMR (62.9 MHz, $CDCl_3$/TMS) δ (ppm): 10.9, 22.1, 110.2, 119.5, 124.0, 124.4, 141.3, 150.8, 168.1.

2-ethyl-1,3-benzothiazole (3o): Yield 85 %, pale yellowish liquid. IR (neat): $\overline{V}$ = 3,060, 2,970, 2,930, 1,520, 1,430, 1,120, 945, 755 cm^{-1}. ^{1}H-NMR (250 MHz, $CDCl_3$/TMS) δ (ppm): 1.17 (t, J = 7.56, 2.25 Hz, 3H), 2.85 (q, J = 7.5, 2.3 Hz, 2H), 6.99–7.18 (m, 2H), 7.53 (d, J = 8.0 Hz, 1H), 7.72 (d, J = 8.0 Hz, 1H). ^{13}C-NMR (62.9 MHz, $CDCl_3$/TMS) δ (ppm): 13.7, 27.7, 121.4, 122.4, 124.6, 125.8, 135.0, 153.2, 173.4.

2-(2-chlorophenyl)-1,3-benzothiazole (3p): Yield 91 %, white solid, mp: 82–83 °C (Lit. [53] mp 82 °C). IR (KBr): $\overline{V}$ = 3,050, 1,480, 1,425, 1,060, 960, 750, 721 cm^{-1}. ^{1}H NMR (250 MHz, $CDCl_3$/TMS) δ (ppm): 7.15–7.37 (m, 5H), 7.73 (d, J = 7.95 Hz, 1H), 7.98 (d, J = 8.0 Hz, 1H), 8.05 (m, 1H). ^{13}C-NMR (62.9 MHz, $CDCl_3$/TMS) δ (ppm): 121.4, 122.9, 125.01, 125.89, 126.3, 130.8, 131.1, 131.76, 132.22, 132.70, 136.12, 152.50, 164.03.

2-(2-chlorophenyl)-1,3-benzoxazole (3q): Yield 90 %, white solid, mp: 65–67 °C. IR (KBr): $\overline{V}$ = 3,060, 1,595, 1,540, 1,440, 1,425, 1,240, 1,020, 810, 730 cm^{-1}. ^{1}H-NMR (250 MHz, $CDCl_3$/TMS) δ (ppm): 7.13–7.23 (m, 4H), 7.30–7.41 (m, 2H), 7.64–7.71 (m, 1H), 7.92–7.99 (m, 1H). ^{13}C-NMR (62.9 MHz, $CDCl_3$/TMS) δ (ppm): 110.7, 120.4, 124.6, 125.5, 126.1, 126.8, 131.3, 131.5, 131.7, 133.4, 141.7, 150.5, 160.8.

2-(2-chlorophenyl)benzimidazole (3r): Yield 92 %, white solid, mp: 234.5 °C (Lit. [56] mp 234 °C). IR (KBr): $\overline{V}$ = 3,445, 3,050, 1,440, 1,400, 1,050, 740 cm^{-1}. ^{1}H-NMR (250 MHz, DMSO-d_6/TMS) δ (ppm): 7.20–7.24 (m, 2H), 7.48–7.51 (m, 2H), 7.54–7.68 (m, 3H), 7.89–7.93 (m, 1H), 12.74 (s, 1H). ^{13}C-NMR (62.9 MHz, DMSO-d_6/TMS) δ (ppm): 111.7, 119.0, 121.7, 122.7, 127.3, 129.9, 130.3, 131.1, 131.6, 132.0, 134.6, 143.1, 149.1.

2-(2,6-difluorophenyl)-1,3-benzothiazole (3 s): Yield 88 %, white solid, mp: 73–74 °C. IR (KBr): 3,070, 1,620, 1,580, 1,465, 1,240, 1,010, 960, 760, 720 cm^{-1}. ^{1}H-NMR (250 MHz, $CDCl_3$/TMS) δ (ppm): 7.03–7.12 (m, 2H), 7.37–7.57 (m, 3H), 7.96 (d, J = 8.1 Hz, 1H), 8.19 (d, J = 7.9 Hz, 1H). ^{13}C-NMR (62.9 MHz, $CDCl_3$/TMS) δ (ppm): 112.2, 121.3, 123.8, 125.7, 126.3, 131.8, 135.6, 153.0, 158.4, 162.5.

2-(2-pyridinyl)benzimidazole (3t): Yield 87 %, pale yellow crystals, mp: 218.5 °C (Lit. [56] mp 218 °C). IR (KBr): 3,450, 3,055, 1,590, 1,440, 1,400, 1,315, 1,280, 1,120, 745 cm^{-1}. ^{1}H NMR (250 MHz, DMSO-d_6/TMS) δ (ppm): 7.16–7.24 (m, 2H), 7.47–7.71 (m, 3H), 7.98 (td, J = 7.7, 1.7 Hz, 1H), 8.30–8.34 (m, 1H), 8.71 (d, J = 6.9 Hz, 1H), 13.01 (s, 1H). ^{13}C-NMR (62.9 MHz, DMSO-d_6/TMS) δ (ppm): 112.0, 119.2, 121.4, 121.9, 123.1, 124.6, 134.8, 137.5, 143.7, 148.4, 149.3, 150.7.

2-(2,6-dichlorophenyl)-1H-1,3-benzimidazole (3u): Yield 88 %, white solid, mp: 279 °C (Lit. [56] mp 218 °C). IR (KBr): 3,430, 3,060, 1,550, 1,430, 1,330, 780, 740 cm^{-1}. ^{1}H-NMR (250 MHz, DMSO-d_6/TMS) δ (ppm): 7.11–7.30 (m, 5H), 7.54 (m, 2H). ^{13}C-NMR (62.9 MHz, DMSO-d_6/TMS) δ (ppm): 115.4, 122.2, 128.3, 130.4, 132.4, 135.0, 137.0, 146.6.

2-(4-bromophenyl)-1,3-benzoxazole (3v): Yield 91 %, white solid, mp: 157–159 °C (Lit. [57] mp 157–158 °C). IR (KBr): 3,050, 1,605, 1,590, 1,480, 1,450, 1,395, 1,240, 1,070, 1,005, 829, 739 cm^{-1}. ^{1}H-NMR (250 MHz, $CDCl_3$/TMS) δ (ppm): 7.29–7.36 (m, 2H), 7.48–7.55 (m, 1H), 7.60 (d, J = 8.55 Hz, 2H), 7.70–7.77 (m, 1H), 8.1 (d,

$J = 8.55$ Hz, 2H). ^{13}C-NMR (62.9 MHz, $CDCl_3$/TMS) δ (ppm): 110.6, 120.1, 124.7, 125.3, 126.0, 126.2, 128.9, 132.2, 141.9, 150.7, 162.0.

2-(4-bromophenyl)-1,3-benzothiazole (3w): Yield 93 %, white solid, mp: 133–134 °C. IR (KBr): 3,050, 1,470, 1,430, 1,390, 1,063, 962, 827, 752, 715 cm^{-1}. ^{1}H NMR (250 MHz, $CDCl_3$/TMS) δ (ppm): 7.21–7.45 (m, 4H), 7.63–7.78 (m, 3H), 7.81 (d, $J = 8.1$ Hz, 1H). ^{13}C-NMR (62.9 MHz, $CDCl_3$/TMS) δ (ppm): 121.6, 123.3, 123.7, 125.4, 126.3, 128.8, 132.2, 132.4, 135.0, 154.0, 166.6.

2-(4-chlorophenyl)benzimidazole (3x): Yield 93 %, white solid, mp: 301–302 °C (Lit. [58] mp 301 °C). IR (KBr): 3,050, 1,650, 1,490, 1,470, 1,430, 1,320, 1,275, 1,090, 1,015, 965, 830, 745 cm^{-1}. ^{1}H-NMR (250 MHz, DMSO-d_6/TMS) δ (ppm): 7.18-7.21 (m, 2H), 7.60 (m, 4H), 8.17 (d, $J = 8.6$ Hz, 2H), 12.99 (s, 1H). ^{13}C-NMR (62.9 MHz, DMSO-d_6/TMS) δ (ppm): 111.4, 118.9, 121.9, 122.7, 128.1, 129, 134.5 150.1.

2-benzyl-1,3-benzothiazole (3y): Yield 88 %, pale yellow liquid. IR (neat): 3,060, 3,030, 2,910, 1,505, 1,430, 1,110, 760 cm^{-1}. ^{1}H-NMR (250 MHz, $CDCl_3$/TMS) δ (ppm): 4.18 (s, 2H), 7.02–7.22 (m, 7H), 7.49 (d, $J = 7.91$ Hz, 1H), 7.82 (d, $J = 8.1$ Hz, 1H). ^{13}C-NMR (62.9 MHz, $CDCl_3$/TMS) δ (ppm): 40.6, 121.6, 122.8, 124.9, 126.0, 127.6, 128.9, 129.0, 135.7, 137.3, 153.4, 171.1.

2-(4-methylphenyl)benzimidazole (3y): Yield 90 %, white solid, mp: 276.5 °C (Lit. [59] mp 275–276 °C). IR (KBr): 3,450, 3,095, 2,980, 2,920, 1,550, 1,500, 1,460, 1,430, 1,390, 1,270, 965, 822, 744. ^{1}H-NMR (250 MHz, DMSO-d_6/TMS) δ (ppm): 2.35 (s, 3H) 7.15–7.20 (m, 2H), 7.33(d, $J = 8.1$ Hz, 2H), 7.46–7.56 (m, 2H), 8.07 (d, $J = 8.1$ Hz, 2H), 12.84 (s, 1H). ^{13}C-NMR (62.9 MHz, DMSO-d_6/TMS) δ (ppm): 20.9, 121.9, 126.3, 127.4, 128.9, 129.4, 139.5, 151.3.

Conclusion

In conclusion, magnetic nanoparticles-supported tungstosilicic acid is reported as a highly efficient and reusable solid acid catalyst for the synthesis of benzoazoles via the reaction of aldehydes and 2-aminophenol, 2-aminothiophenol or benzene-1,2-diamine in water. The catalyst showed high activity in this process and desired products were obtained in high yields under green conditions in relatively short reaction time. For this process, TSAMNP acts as a heterogeneous catalyst and can be recovered from the reaction mixture using external magnetic field. TSAMNP was reused for 6 runs without significant lose in its catalytic activity.

Acknowledgments We would like to thank financial support of Iran National Science Foundation (INSF)-Grant no. 88001894. Also the financial supports of research councils of Shiraz University are gratefully acknowledged.

References

1. K.T.V. Rao, P.S.S. Prasad, N. Lingaiah, Green. Chem. **14**, 1507 (2012)
2. E. Rafiee, M. Joshaghani, S. Eavani, S. Rashidzadeh, Green. Chem. **10**, 982 (2008)
3. N. Azizi, L. Torkiyan, M.R. Saidi, Org. Lett. **8**, 2079 (2006)
4. A. Khalafi-Nezhad, F. Panahi, B. Golesorkhi, Helv. Chim. Acta. **96**, 1155 (2013)
5. A. Khalafi-Nezhad, M. Divar, F. Panahi, Tetrahedron Lett. **54**, 220 (2013)
6. T. Ueda, H. Kotsuki, Heterocycles **76**, 73 (2008)
7. F.M. Zhang, J. Wang, C.S. Yuan, X.Q. Ren, Catal. Lett. **102**, 171 (2005)
8. V. Brahmkhatri, A. Patel, Ind. Eng. Chem. Res. **50**, 13693 (2011)
9. G. Kamalakar, K. Komura, Y. Kubota, Y. Sugi, J. Chem. Technol. Biotechnol. **81**, 981 (2006)
10. B. Karami, V. Ghashghaee, S. Khodabakhshi, Catal. Commun. **20**, 71 (2012)
11. P.D. Stevens, J.D. Fan, H.M.R. Gardinmalla, M. Yen, Org. Lett. **7**, 2085 (2005)
12. A. Khalafi-Nezhad, F. Panahi, S. Mohammadi, H.O. Foroughi, J. Iran. Chem. Soc. **10**, 189 (2013)
13. T Hyeon, Chem. Commun. (8), 927–934 (2003)
14. S. Shylesh, J. Schweizer, S. Demeshko, V. Schnemann, S. Ernst, W.R. Thiel, Adv. Synth. Catal. **351**, 1789 (2009)
15. H. Hamadi, M. Kooti, M. Afshari, Z. Ghiasifar, N. Adibpour, J. Mol. Catal. A. Chem. **373**, 25 (2013)
16. J.N. Plampin, C.K. Cain, J. Med. Chem. **6**, 247 (1963)
17. G.L. Dunn, P. Actor, V.J. DiPasquo, J. Med. Chem. **9**, 751 (1966)
18. X.-W. Sun, S. Neidleb, J. Mann, Tetrahedron Lett. **43**, 7239 (2002)
19. Neidle S, Rayner EL, Simpson IJ, Smith NJ, Mann J, Baron A, Opoku-Boahen Y, Fox KR, Hartley JA, Kelland LR, Chem. Commun. (10), 929–930 (1999)
20. C.L. Sann, A. Baron, J. Mann, H.V.D. Berg, M. Gunaratnam, S. Neidle, Org. Biomol. Chem. **4**, 1305 (2006)
21. M.A. Estiarte, R.J. Johnson, C.J. Kaub, S. Gowlugari, D.J.R. O'Mahony, M.T. Nguyen, D.E. Emerling, M.G. Kelly, J. Kincaid, F. Vincent, M.A. Duncton, J. Med. Chem. Commun. **3**, 611 (2012)
22. S.T. Huang, I.J. Hsei, C. Chen, Bioorg. Med. Chem. **14**, 6106 (2006)
23. J. Pérez-Villanueva, R. Santos, A. Hernández-Campos, M.A. Giulianotti, R. Castillo, J.L. Medina-Franco, Med. Chem. Commun. **2**, 44 (2011)
24. J. Kuwabara, T. Namekawa, M. Haga, T. Kanbara, Dalton. Trans. **41**, 44 (2012)
25. D. Yao, S. Zhao, J. Guo, Z. Zhang, H. Zhang, Y. Liu, Y. Wang, J. Mater. Chem. **21**, 3568 (2011)
26. S. Dey, P. Vivo, A. Efimov, H. Lemmetyinen, J. Mater. Chem. **21**, 15587 (2011)
27. C. Cojocariu, P. Rochon, J. Mater. Chem. **14**, 2909 (2004)
28. W. Ai, W. Zhou, Z. Du, Y. Du, H. Zhang, X. Jia, L. Xie, M. Yi, T. Yu, W. Huang, J. Mater. Chem. **22**, 23439 (2012)
29. H.-J. Lim, D. Myung, I.Y.C. Lee, M.H. Jung, J. Comb. Chem. **10**, 501 (2008)
30. K. Bahrami, M.M. Khodaei, A. Nejati, Green. Chem. **12**, 1237 (2010)
31. C.O. Kangani, D.E. Kelley, B.W. Day, Tetrahedron Lett. **47**, 6497 (2006)

32. W.-J. Yoo, H. Yuan, H. Miyamura, S. Kobayashi, Adv. Syn. Catal. **353**, 3085 (2011)
33. J. Bonnamour, C. Bolm, Org. Lett. **10**, 2665 (2008)
34. Kantam ML, Venkanna GT, Kumar KBS, Balasurbrahmanyam V, Bhargava S, Synlett. (11), 1753–1756 (2009)
35. A. Srivani, K.T. Venkateswar Rao, P.S. Sai Prasad, N. Lingaiah, J. Mol. Catal. A. Chem. **328**, 119 (2010)
36. Y.-X. Chen, L.-F. Qian, W. Zhang, B. Han, Angew. Chem. Int. Ed. **47**, 9330 (2008)
37. T. Okitsu, K. Nagase, N. Nishio, A. Wada, Org. Lett. **14**, 708 (2012)
38. P. Ren, I. Salihu, R. Scopelliti, X. Hu, Org. Lett. **14**, 1748 (2012)
39. P.J. Boissarie, Z.E. Hamilton, S. Lang, J.A. Murphy, C.J. Suckling, Org. Lett. **13**, 6256 (2011)
40. A. Teimouri, A.N. Chermahini, H. Salavati, L. Ghorbanian, J. Mol. Catal. A. Chem. **373**, 38 (2013)
41. K. Bahrami, M.M. Khodaei, F. Naali, J. Org. Chem. **73**, 6835 (2008)
42. Bahrami K, Khodaei MM, Naali F, Synlett. 569 (2009)
43. Bahrami K, Khodaei MM, Kavianinia I, Synthesis 417–427 (2007)
44. W.-G. Huang, D.-H. He, J.-Y. Liu, Q.-M. Zhu, Appl. Catal. A. Gen. **199**(1), 93–98 (2000)
45. D. Yuan, Q. Zhang, J. Dou, Catal. Commun. **11**, 606 (2010)
46. Y. Kang, L. Zhou, X. Li, J. Yuan, J. Mater. Chem. **21**, 3704 (2011)
47. M. Nasr-Esfahani, M. Montazerozohori, T. Gholampour, Bull. Korean Chem. Soc. **31**, 3653 (2010)
48. Sharghi H, Beyzavi MH, Doroodmand MM (2008) Eur. J. Org. Chem. 4126
49. T. Okuhara, N. Mizuno, M. Misono, Adv. Catal. **41**, 113–252 (1996)
50. C. Wang, H. Daimon, S. Sun, Nano. Lett. **9**, 1493 (2009)
51. P. Gogoi, D. Konwar, Tetrahedron Lett. **47**, 79 (2006)
52. H. Xiangming, M. Huiqiang, W. Yulu, Arkivoc **8**, 150 (2007)
53. M. Kodomari, Y. Tamaru, T. Aoyama, Synth. Commun. **34**, 3029 (2004)
54. Y. Kawashita, C. Ueba, M. Hayashi, Tetrahedron Lett. **47**, 4231 (2006)
55. M.I. El-Sheikh, A. Marks, E.R. Biehl, J. Org. Chem. **46**, 3256 (1981)
56. A.B. Alloum, K. Bougrin, M. Soufiaoui, Tetrahedron Lett. **44**, 5935 (2003)
57. G. Evindar, R.A. Batey, J. Org. Chem. **71**, 1802 (2006)
58. V.I. Cohen, J. Heterocycl. Chem. **14**, 1321 (1977)
59. B. George, E.P. Papadopoulos, J. Org. Chem. **42**, 441 (1977)